Cold Regions Science and Technology, 17 (1989) 61–76
Elsevier Science Publishers B.V., Amsterdam — Printed in The Netherlands

BREAKUP OF ANTARCTIC FAST ICE

G.B. Crocker[1] and P. Wadhams
Scott Polar Research Institute, University of Cambridge, Lensfield Road, Cambridge CB2 1ER (England)

(Received June 17, 1988; revised and accepted February 5, 1989)

ABSTRACT

The fast ice cover in McMurdo Sound, Antarctica, is subjected to numerous mechanical processes which are capable of inducing breakup. Thermal decay plays only a minor role in the destruction of the ice cover, making this region ideal for studying mechanical breakup processes without the complications caused by melting and internal deterioration. A previously developed thermodynamic ice-growth model is used to predict temporal changes in the physical properties of the ice sheet relevant to breakup, allowing the susceptibility of the ice to different destructive processes to be assessed on a seasonal basis. The analyses indicate that during most of the year wind-induced tensile failure is the only likely mode of fracture, while during the short summer period ocean swell incident on the fast ice edge becomes dominant. The importance of the pack ice cover in the Ross Sea in controlling breakup by attenuating potentially destructive ocean swell is clearly shown, and is in agreement with previous qualitative studies of fast ice breakup.

INTRODUCTION

At its peak extent in late winter, Antarctic fast ice covers a sea surface area of roughly 5.5×10^5 km^2 (Panov and Fedotov, 1979). Although this is small in comparison to the 2.0×10^7 km^2 of pack ice in the Southern Ocean at the same time of year (Zwally et al., 1983), its distribution around the coastline of the Antarctic continent makes it of considerable importance to shore-based logistic operations. Most Antarctic fast ice is seasonal, and in contrast to fast ice in the Arctic, undergoes little or no surface melting or internal deterioration during the summer, particularly in the more southerly regions. Basal melting can result in some thinning of the ice cover, but its destruction is primarily the result of mechanical processes. This makes the Antarctic fast ice zone an ideal area for investigating the mechanics of breakup, without many of the complications introduced by thermal deterioration. In this paper we present a theoretical analysis of the breakup of the fast ice cover in McMurdo Sound, Antarctica (Fig. 1), incorporating observations and measurements of ice properties, thermodynamics, and wave dynamics in McMurdo Sound during the austral winter of 1986 (Crocker, 1988).

A thermodynamic ice growth model developed specifically for McMurdo Sound, and incorporating the contributions to growth of snow-ice and sub-ice platelet formations (Crocker, 1988; Crocker and Wadhams, 1989) is used to predict the physical properties of the ice sheet over the course of a single growth and decay cycle, which are then used in conjunction with existing empirical formulae to estimate the mechanical ice properties relevant to the problem of ice breakup. By comparing the forces required to induce breakup by any specific mechanism, or combination of mechanisms, with the environmental conditions required to produce these forces and the likelihood of these conditions occurring, we then assess the seasonal variations in the susceptibility of the ice sheet to breakup, and dis-

[1]Present address: Centre for Cold Ocean Resources Engineering, Memorial University of Newfoundland, St. John's, Nfld (Canada).

0165-232X/89/$03.50

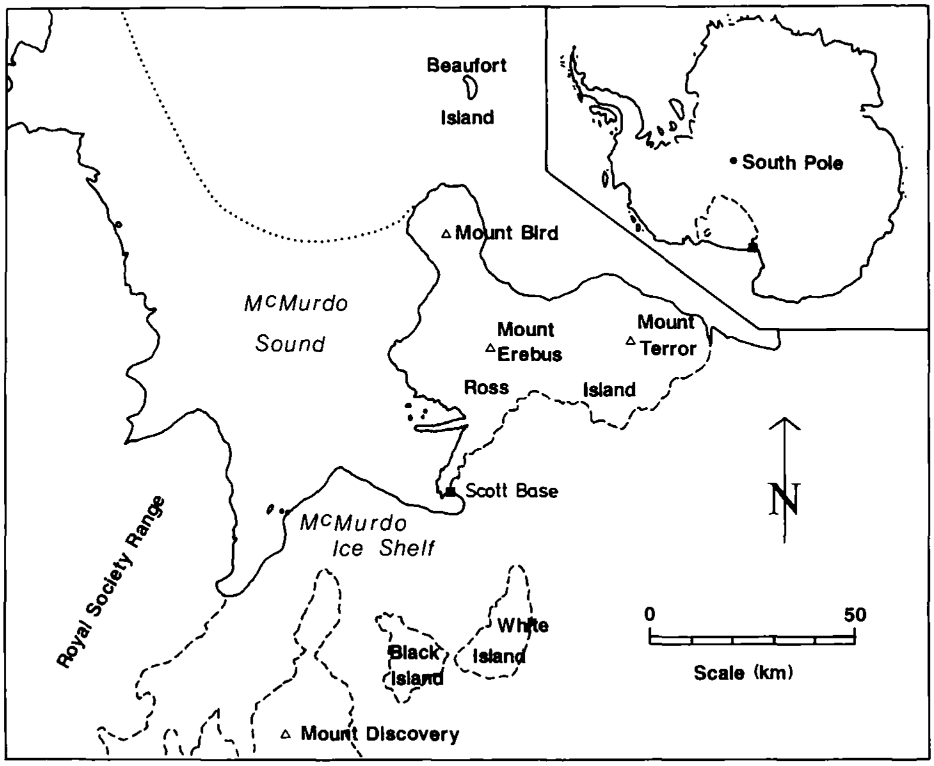

Fig. 1. Map of the McMurdo Sound region. The dotted line indicates the approximate position of the fast ice edge at the end of winter maximum.

cuss the predictions with reference to observed patterns of breakup in McMurdo Sound.

THE PHYSICAL AND MECHANICAL PROPERTIES OF MCMURDO SOUND FAST ICE

The thermodynamic model used is a modified version of the Semtner (1976) model and has been shown to produce reasonable estimates of ice growth in McMurdo Sound (Crocker, 1988; Crocker and Wadhams, 1989). In the following analyses one complete seasonal cycle, beginning on the day the ice sheet first forms (assumed to be March 1) and ending 365 days later, will be examined. The exact form of the model and the input parameters used are as described in Crocker (1988), and the predicted total ice thickness is shown in Fig. 2. Here "total" thickness refers to snow-ice, and ice formed by the inclusion of sub-ice platelets, as well as columnar ice. It is assumed that all three of these ice types have the same mechanical properties. This is not a strictly valid assumption, considering how much variation exists in their crystal structures, densities, and brine volumes, but very little is known about the mechanical properties of snow and platelet ice. The effects of grain size, salinity, pore space, and crystal structure on ice strength are not well enough understood to allow predictions of the strengths of snow-ice and ice formed by columnar growth into a sub-ice platelet layer. In the absence of direct measurements, we must assume that they can be adequately defined by relationships derived for columnar sea ice.

Taking the predicted snow surface temperature (T_0), the temperature at the base of the ice sheet (T_B), and the predicted conductive flux through the snow and ice slab (F_c), and assuming that the flux through the ice is equal to the flux through the slab, the mean ice temperature ($\bar{T}$) can be calculated:

$$\bar{T}=\left(\frac{h_i F_c}{k_i}+2T_B\right)\Big/2 \quad (1)$$

Since the salinity measurements from the 1986 field season are limited to the relatively thick multi-year ice in the southern end of McMurdo Sound, the temporal changes in S for a complete growth cycle can only be estimated. On the basis of previous studies, primarily on Arctic sea ice (Cox and Weeks, 1974, for example), and the few salinity measurements performed in this study, a logarithmic desalination curve of the form:

$$S=-4\log t+16 \quad (2)$$

is used, where t is the number of days after freeze-up and S is salinity in parts per thousand. This formula reflects both the high initial salinity, and the comparatively high equilibrium values found in Antarctic sea ice. From $\bar{T}$ and S, the equations of Frankenstein and Garner (1967) are used to calculate the mean brine volume (ν_b), which is in turn used in the empirical equation:

$$E/E_0=(1-\nu_b^{1/2})^4 \quad (3)$$

(where E_0 is Young's modulus for pure ice) to derive an estimate of Young's modulus (E).*

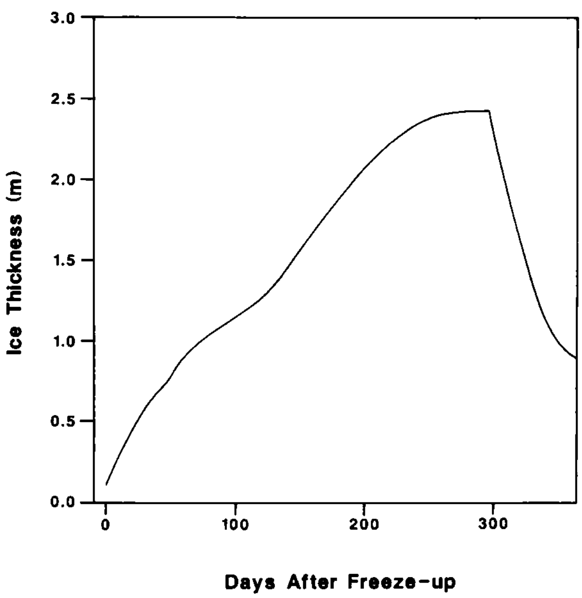

Fig. 2. Predicted ice thickness for a 365 day period after a March 1st freeze-up.

The results of these calculations are summarized in Fig. 3, along with the tensile strength of the ice (σ^*). Tensile strength can be estimated using the Griffith criterion for mode I fracture (Mellor, 1983). By equating the change of potential energy in the plate to the change in the surface energy in a pre-existing crack of length (c_r) as the crack grows in length, the tensile stress (applied perpendicular to the long axis of the crack) necessary to induce crack propagation can be defined as:

$$\sigma^*=(2E\gamma^*/\pi c_r)^{1/2} \quad (4)$$

where γ^* is the specific surface energy of the ice (≈ 0.1 J m^{-2}). The crack size is normally assumed to be equal to the size of the individual ice grains, roughly 0.01 m. Clearly the estimate of σ^* is highly dependent on the values chosen for c_r and γ^*, which are not known to any degree of certainty. The specific surface energy in particular is difficult to quantify, and there is some evidence to suggest that γ^* should be replaced by a term γ_p^* which includes the specific energy for plastic working, where $\gamma_p^* \gg \gamma^*$ (see Mellor, 1983). An alternative method of calculating σ^* is to use fracture mechanics theory (Goodman et al., 1980). Using a critical stress intensity factor (K_{Ic}), the critical surface strain can be calculated as:

$$\epsilon^*=K_{Ic}\frac{1-\nu^2}{\Omega E\sqrt{\pi c_r}} \quad (5)$$

*There are large differences among the values of Young's modulus produced by various empirical formulae. Equation 3 is from Schwarz and Weeks (1977), and was chosen because it produced results in good agreement with the only available values of E for McMurdo Sound fast ice (derived from vehicle experiments by Squire et al., 1987). It also yields results similar to the experimental data of Anderson (1958) and Dykins (1971). It has been brought to our attention by A. Assur that the formula as written in Schwarz and Weeks (1977) is erroneous, the correct equation being:

$$E/E_0=(1-\nu_b)^4$$

We have used Eq. 3 to estimate E in the following analyses as it produces reasonable results for McMurdo Sound fast ice over the range of brine volumes encountered, but the reader should be aware of the misprint in the paper by Schwarz and Weeks.

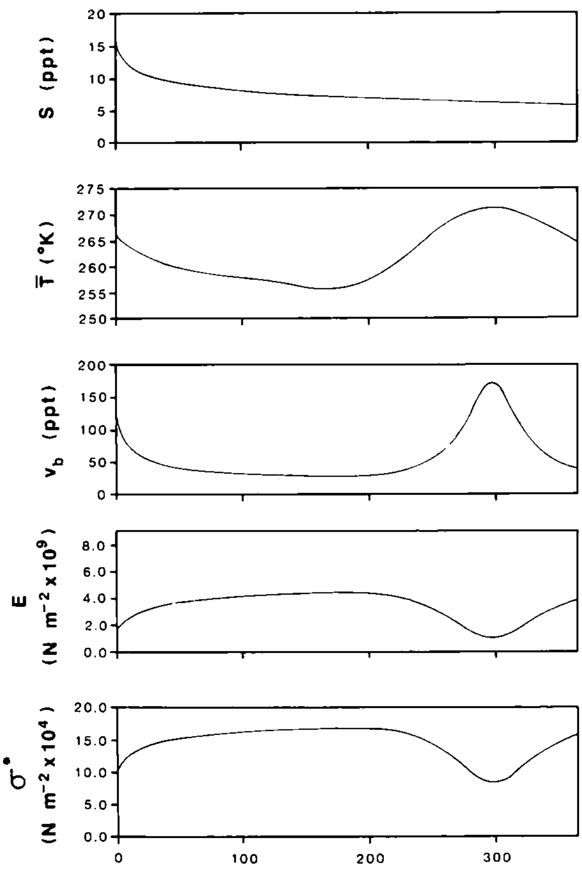

Fig. 3. Predicted seasonal variations in ice salinity (S), mean temperature ($\bar{T}$), brine volume (ν_b), Young's modulus (E), and flexural strength (σ^*).

where Ω is constant roughly equal to one. Since (Wadhams, 1980):

$$\sigma^* = \frac{E\epsilon^*}{(1-\nu^2)} \tag{6}$$

where ν is Poisson's ratio, substitution of Eq. 5 into Eq. 6 yields:

$$\sigma^* = K_{Ic} \frac{1}{\Omega\sqrt{\pi c_r}} \tag{7}$$

Equations 4 and 7 are numerically equivalent since $K_{Ic} = \sqrt{2E\gamma^*}$, but stress intensity is a measurable quantity, permitting calculations of σ^* without having to estimate γ^*. Taking $K_{Ic} = 5\times10^4$ N m$^{-3/2}$ (Goodman et al., 1980), and $E = 4\times10^9$, then by fracture mechanics $\sigma^* = 2.8\times10^5$ and $\epsilon^* = 7.0\times10^{-5}$, while using Eq. 4 we get $\sigma^* = 1.5\times10^5$ and $\epsilon^* = 3.8\times10^{-5}$. Goodman et al. (1980) found by direct field observation, that the fracture strain of a sea ice floe was $\approx 3\times10^{-5}$, a value more compatible with the estimate obtained using the Griffith criterion. However, considering the uncertainties in estimating γ^* and the wide range of experimental measurements of K_{Ic}, it is difficult to make judgements regarding the effectiveness of the two methods. In the absence of a better test, Eq. 4 will be used in the following analyses.

Referring again to Fig. 3, it can be seen that the effects of changes in h_i and υ_b combine to produce minimum tensile strengths when the ice is relatively warm and thin (immediately after formation, and during the summer). Note also that $\bar{T}$ approaches but never reaches T_B, and although there is a considerable increase in brine volume, the ice never completely loses its strength.

BREAKUP BY OCEAN SWELL

The dispersion equation for propagating waves in a continuous ice sheet of uniform thickness over water of finite depth (H) can be written as (Crocker, 1988; Crocker and Wadhams, 1988):

$$Dk_i^5 + \rho_o g k_i - \omega^2(\rho_o \coth(k_i H) + \rho_i k_i h_i) = 0 \tag{8}$$

where k_i is the wave number in ice covered water, ω is the angular frequency, g is the gravitational acceleration, ρ_o and ρ_i are the densities of sea water and sea ice respectively, and the flexural rigidity (D) is defined by:

$$D = \frac{Eh_i^3}{12(1-\nu^2)} \tag{9}$$

Equation 8 has three physically feasible roots, one real representing the propagating wave of interest here, and two complex conjugates representing evanescent edge waves. It should be noted that if an ice cover is subjected to compressive stresses the nature of the dispersion changes. Liu and Mollo-Christensen (1988) have performed a theoretical analysis of the effects of compressive stress on wave propagation through a pack ice cover and found that the resulting reduction in the group velocity can lead to large local concentrations of wave energy. They use this finding to explain the presence of large long-period waves deep in the pack ice zone of the Weddell Sea (see Wadhams et al., 1987), and similar conditions may have a bearing on the swell propagation analyses described below, but at the present time the importance of this process cannot be adequately assessed.

In order to assess the susceptibility of an ice sheet to breakup by wave action, we must be able to define a critical wave amplitude (a_i^*) at which the surface strain is equal to the fracture strain. From the theory of elastic bending the tensile stress at the ice surface can be defined as (Carter et al., 1981):

$$\sigma^* = \frac{2\pi E h_i a_i^*}{\lambda_i^2 (1-\nu^2)} \tag{10}$$

Rearranging for a_i^* gives:

$$a_i^* = \frac{\sigma^* \lambda_i^2 (1-\nu^2)}{2\pi E h_i} \tag{11}$$

where λ_i is found by solving the dispersion equation, and σ^* comes from Eq. 4. Assuming for the moment that 100% of the energy contained in an open-water wave incident on an ice edge is transmitted into the ice covered region, then the critical open-water wave amplitude of the incident swell (a_o^*) is:

$$a_o^* = \frac{\sigma^* \lambda_i^2 (1-\nu^2)}{2\pi E h_i} \frac{a_o}{a_i} \tag{12}$$

where the ratio a_o/a_i is determined using (Crocker, 1988):

$$\frac{a_o}{a_i} = \frac{U_i}{U_o} \left[1 + \frac{E h_i^3 k_i^4}{12(1-\nu^2)\rho_w g} \right] \tag{13}$$

The group velocity in ice covered water (U_i) is defined by:

$$U_i = C_i - \lambda_i \frac{\partial C_i}{\partial \lambda_i} \tag{14}$$

and the phase velocity in ice covered water is:

$$C_i = \lambda_i / T \tag{15}$$

where T is the wave period. The group velocity in open water can be calculated using:

$$U_o = \frac{1}{2} C_o \left(1 + \frac{2k_o H}{\sinh 2k_o H} \right) \tag{16}$$

and (Defant, 1961):

$$C_o = \left(\frac{g}{k_o} \tanh k_o H \right)^{1/2} \tag{17}$$

A method for determining the energy ($|R|^2$) and amplitude ($|R|$) reflection coefficients by surface matching velocity potentials across the open water and ice covered regions is outlined in Wadhams (1986), and the reader should refer to this publication for a complete description. For a single reflection across a fast ice edge the amount of energy reflected is generally small, although at short periods and in thick ice the losses can be substantial. The temporal variations in a_i^* and a_o^* predicted using the ice properties generated by the thermodynamic model, and including the effects of energy reflection, are shown in Figs. 4 and 5 for a range of wave periods. There is a rapid decrease in both a_i^* and a_o^* immediately after freeze-up, as the thin, flexible mat quickly thickens and hardens. Later in the season the pattern is more complex and difficult

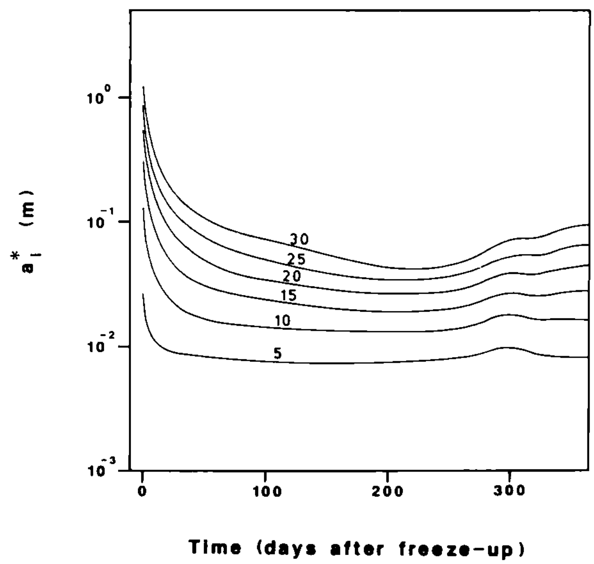

Fig. 4. Seasonal variations of the in-ice wave amplitude required to fracture the ice sheet (a_i^*) for wave periods of 5, 10, 15, 20, 25, and 30 s.

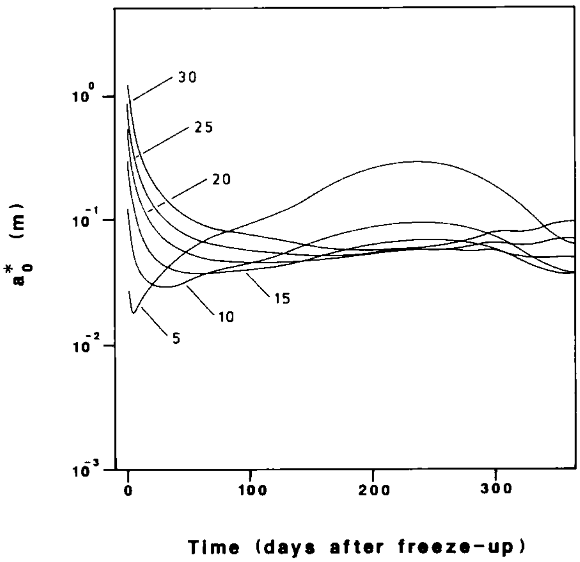

Fig. 5. Seasonal variations of the open water wave amplitude required to fracture the ice sheet (a_o^*) for wave periods of 5, 10, 15, 20, 25, and 30 s.

to explain. The curves indicate that in mid-winter when the ice is thickest and strongest, a_i^* reaches a minimum, as does a_o^* at long periods. In the summer, as h_i and σ^* are reduced, the wave amplitude necessary to induce fracture *increases*. This is in direct contrast to what might be expected intuitively, but can be explained by looking at the way in which the wave energy is partitioned between the flexural wave in the ice and the gravity wave in the water. After Wadhams (1973a), and Carter et al. (1981), we can define the components of the kinetic and potential energies of the ice and underlying water as:

(a) the average kinetic energy of the water per unit surface area:

$$E_1 = \frac{\rho_w \omega^2}{4k_i} a_i^2 \coth(k_i H) \tag{18}$$

(b) the average potential energy stored in the water per unit surface area:

$$E_2 = \rho_w g a_i^2 / 4 \tag{19}$$

(c) the average kinetic energy of the ice per unit surface area:

$$E_3 = \omega^2 \rho_i h_i a_i^2 / 4 \tag{20}$$

(d) the average potential energy of the ice per unit surface area:

$$E_4 = \frac{E h_i^3 k_i^4 a_i^2}{48(1-\nu^2)} \tag{21}$$

Figure 6 shows the total kinetic and potential energies of waves in the ice/water system, the sum of Eqs. 18–21. Again we see that the *total* wave energy required to fracture the ice is greatly reduced in mid-winter. However, Fig. 7 reveals that the energy contained in the ice at amplitudes equal to a_i^* does in fact increase as the ice increases in thickness and strength. In effect, ice-coupled waves, travelling through thick ice with a high tensile strength, propagate with a greater proportion of the total wave energy in the ice than do those propagating through thin, more flexible ice sheets. Most importantly, this increased proportion of total wave energy is sufficiently large to overcome the increased absolute energy required to induce fracture, and allows smaller, lower energy waves to produce the critical surface strain. In other words, the ice is most susceptible to breakup by long period waves in mid-winter when it is thickest and strongest (see Assur, 1963). This is an important finding, as it will be shown below that the waves most likely to reach the fast ice edge

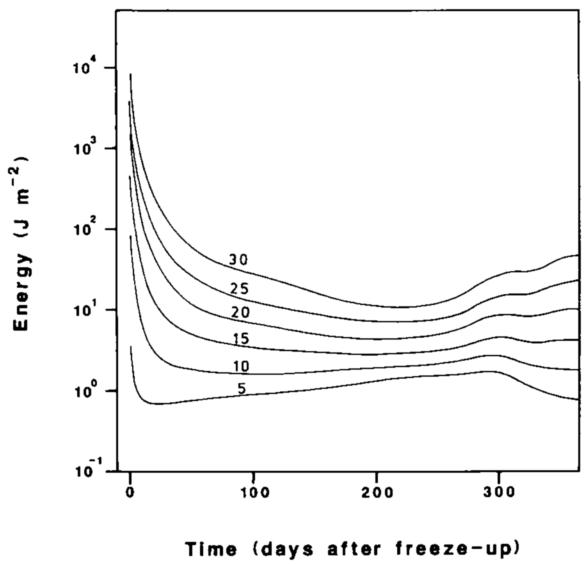

Fig. 6. Seasonal variations of the total potential and kinetic wave energies ($E_1+E_2+E_3+E_4$) contained in waves of amplitude a_i^* and periods of 5, 10, 15, 20, 25, and 30 s.

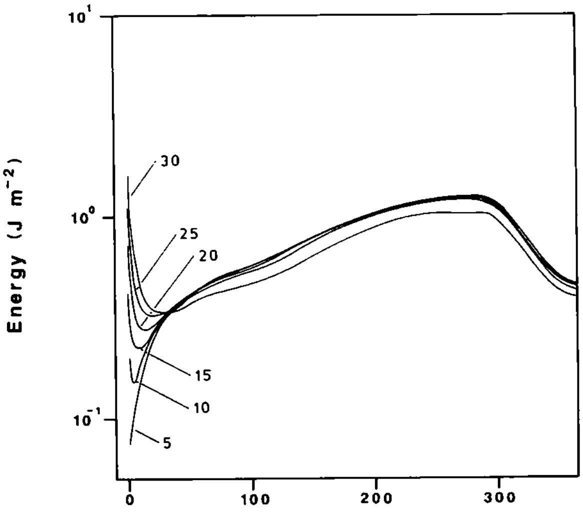

Fig. 7. Seasonal variations of the total potential and kinetic energies in the in-ice portion (E_3+E_4) of an ice-coupled wave of amplitude a_i^* and periods of 5, 10, 15, 20, 25, and 30 s.

in mid-winter are those with the longest periods.

Again referring to Figs. 4 and 5, several additional features are noteworthy. Throughout the season values of a_i^* for waves with periods of 5 s are consistently about one order of magnitude lower than those with 30 s periods. This is simply because short period waves produce greater surface curvatures, and therefore greater surface strains, than long period waves of comparable amplitude. In fact, this effect is greatly reduced here because of the influence of the shallow water (290 m) on the dispersion relation at long periods. Values of a_i^* shown in Fig. 4 are more than one order of magnitude lower than they would be for the same ice sheet over deep water.

A similar early season pattern can be seen in Fig. 5, when the thin, flexible ice has a minimal effect on waves travelling across the ice edge. This similarity quickly disappears as the ice thickens, with a_0^* dramatically increasing for short period waves, although the longer waves do not "feel" the ice as much. The absolute values of the critical wave amplitudes are also interesting. In mid-winter, waves of any period with amplitudes larger than about 0.2 m will induce fracture. In the open ocean, waves of this magnitude are virtually always present, indicating that in the absence of a protective pack ice belt, a stable fast ice cover could not develop. Ice conditions in the Ross Sea therefore appear to play a vital role in controlling the growth and destruction of the fast ice in McMurdo Sound, but before looking at the effect of the pack ice in the Ross Sea on swell attenuation and fast ice breakup, we must first find a representative incident open-ocean wave spectrum. In the general absence of observational wave data in this region in winter, we use the Pierson and Moskowitz (1964) power spectrum for a fully developed sea, where the frequency-dependent energy density ($E(f)$) is given by:

$$E(f)=\alpha g^2(2\pi)^{-4}f^{-5}\exp\left[-\frac{5}{4}\left(\frac{f_m^4}{f}\right)\right] \qquad (22)$$

where α is a constant (8.1×10^{-3}), and f_m is the frequency of peak energy ($0.14\times g/u$, where u is the mean wind velocity in m s^{-1}). The only unknown in the formula is the mean wind velocity, which will be set to 25 m s^{-1} in the following calculations (see Mognard et al., 1983), although the effects of higher and lower mean wind speeds will also be considered. The spectral energy densities produced by the Pierson-Moskowitz formula for mean wind velocities of 20, 25, and 30 m s^{-1}, are plotted in Fig. 8.

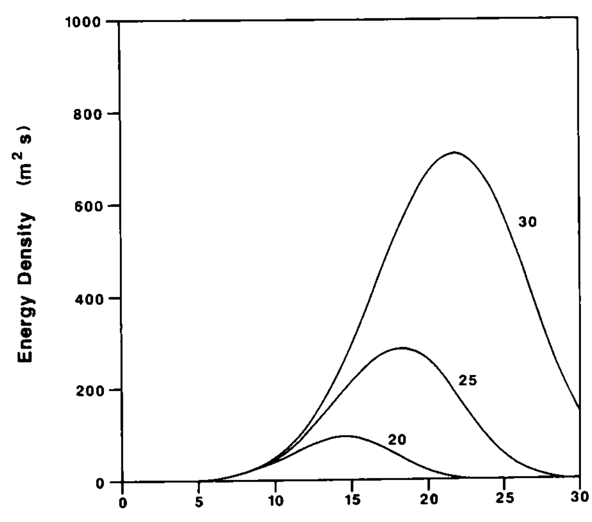

Fig. 8. Pierson and Moskowitz (1964) power energy density spectra for a fully developed sea, with mean wind velocities of 20, 25, and 30 m s^{-1}.

The extent (x) and concentration (p_i) of the seasonal ice in the Ross Sea have been extracted from satellite passive microwave observations of the Antarctic seas between 1973 and 1976 (Zwally et al., 1983), and are summarized in Table 1. The estimates have been made by eye from the small scale maps contained in the report, and are therefore quite crude, but still provide a general picture of ice conditions which might be expected in the region in an average ice year.

Ice thickness is more difficult to predict, and the paucity of measurements in the Ross Sea in winter means that we can only guess at the temporal nature of the thickness distribution. On the basis of observations from the Weddell Sea in 1986 (Wadhams et al., 1987), where the ice was found to be quite thin (generally less than 1.0 m, even in late winter), values of h_i have been selected, somewhat arbitrarily, and are included in Table 1. It will shown below that the values chosen for h_i, within a plausible range, do not have as great an influence on the results of the analyses as might at first be anticipated.

Once the incident wave spectrum and pack ice conditions have been established, we consider the two mechanisms producing significant energy losses as the waves travel through the pack: scattering and bottom drag (for a complete description of likely energy loss processes the reader should refer to Wadhams, 1973b, and Crocker, 1988). For energy losses due to scattering, the wave energy at a distance x in from the edge of a field of large floes (E_x) can be expressed by:

$$E_x = E_0 \exp(-2\alpha^* x) \tag{23}$$

where E_0 is the wave energy crossing the ice edge, and α^* is the amplitude attenuation coefficient. For a more or less continuous ice cover with leads:

$$\alpha^* \approx n|R|^2 \tag{24}$$

where n is the mean number of leads per unit distance, and in a field of discrete floes:

$$\alpha^* \approx \frac{1}{2} \sum_i \frac{p_i |R|^2}{d_i} \tag{25}$$

where p_i is the fraction of the sea surface occupied by floes of diameter d_i. In the following analyses the ice floe diameter is assumed to be constant at 100 m, and Eq. 25 is used to calculate α^*. Energy losses due to bottom friction have been modelled after Putnam and Johnson (1949) who found that the rate of energy dissipation due to bottom friction (D_f) is:

$$D_f = k_d \frac{4\pi^2 \rho_w}{3T^3} \frac{h_w^3}{(\sinh 2\pi H/\lambda_o)^3} \tag{26}$$

where k_d is a drag coefficient roughly equal to 0.008 (Bagnold, 1947), and h_w is the wave height. Energy losses due to scattering are greatest at short periods, while bottom drag preferentially attenuates long-period wave energy. However, the mean depth of the Ross Sea (≈ 1000 m) is sufficient for D_f to be relatively small at all frequencies, and so it is the ice cover which is responsible for the bulk of the energy loss.

Seasonal estimates of the amplitudes of waves penetrating the pack ice zone and reaching McMurdo Sound, are shown in Fig. 9 for six wave periods ranging from 5 to 30 s. The influence of the pack is immediately evident. Through most of the winter, the only waves reaching the fast ice edge with significant energy are those at the extreme long period end of the gravity wave spectrum. Even the thin, sparse, ice covers present in March and April result in large reductions of wave energy, and only during February, when the pack ice completely disappears, can a complete spectrum of large amplitude waves be expected to reach the fast ice edge. If the floe diameter is reduced to pancake proportions

TABLE 1

Pack ice characteristics in the Ross Sea

Month	Extent (x) (km)	Coverage (p_i)	Thickness (h_i) (m)
March	790	0.36	0.25
April	1280	0.80	0.45
May	1340	0.88	0.75
June	1400	0.88	0.90
July	1450	0.88	1.00
August	1500	0.92	1.00
September	1500	0.88	1.00
October	1450	0.88	1.00
November	1400	0.80	1.00
December	850	0.56	1.00
January	120	0.44	1.00
February	0	0.00	0.00

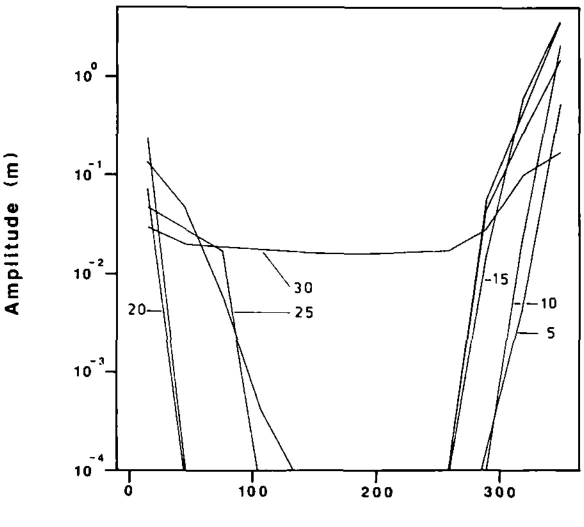

Fig. 9. Predicted amplitudes of waves with periods of 5, 10, 15, 20, 25, and 30 s reaching the fast ice edge in McMurdo Sound over a one year period. The wave spectrum incident on the outer edge of the pack ice zone is that of Pierson and Moskowitz (1964) with a mean wind velocity of 25 m s^{-1}.

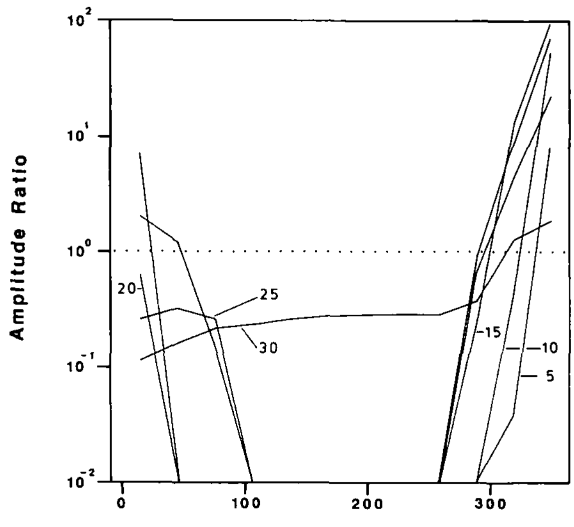

Fig. 10. Seasonal variations in the ratio of the amplitude of swell reaching the fast ice edge to the critical open water wave amplitude (a_o^*), for periods of 5, 10, 15, 20, 25, and 30 s.

(1–5 m) when the ice is thin, a more realistic value than 100 m, then further reductions in propagating wave energy occur at all periods, with the shortest waves experiencing the greatest changes.

In Fig. 10 the ratio of wave amplitude reaching the fast ice edge to the critical wave amplitude (a_o^*) is plotted for waves of the same six periods. Only when the amplitude ratio is greater than or equal to one would fracturing be expected. Here the seasonal effects are again dramatic, with waves of all periods being capable of inducing fracture during the summer, and none of the waves being of sufficient amplitude in winter. Even the 30 s wave, which possesses the most energy and largest amplitude throughout the winter, is almost an order of magnitude too small. The effect of changing the Pierson-Moskowitz spectrum by increasing or decreasing u (within a realistic range) is minimal in terms of ice fracture. When u is 30 m s^{-1} the amplitude ratio for 30 s swell is increased, but remains well below the critical value of one, while reducing u to 20 m s^{-1} causes only a slight reduction in the amplitude ratio at 30 s. The patterns exhibited by waves at the five shorter periods remain virtually unchanged over this wind speed range.

Our discussion of the role of swell in breaking up fast ice sheets has so far dealt solely with propagating flexural-gravity waves, the real root in Eq. 8. However, the two complex roots, representing the evanescent edge waves, combine with the propagating wave to produce a maximum surface strain at a distance of about 30 m ($\pm$10 m) in from the ice edge (Wadhams, 1980; Squire, 1984). As a result, the open water wave amplitude (a_o^*) required to cause tensile failure near the ice edge will be lower than that calculated on the basis of the propagating wave alone. The effect is greatest for short period waves and in thick ice, but the absolute increase in surface strain is relatively small (see Squire, 1984). Therefore, although the edge waves are important in controlling the *pattern* of breakup, they will have little effect on the amplitude ratios shown in Fig. 10. In fact, their importance is further reduced in this case because, except during the summer, the short period waves which produce the greatest edge effects are almost completely attenuated in the pack ice zone.

One way in which the pattern of breakup, resulting from edge wave generation, may influence a_o^* is by the creation of a narrow band of floes at the fast ice edge. Each successive section of fast ice which breaks away under the influence of incident swell acts as a scattering body, and contributes to a reduction in the wave energy reaching the new, receding, fast ice edge. Simple calculations using Eqs. 23 and 25 show that a 10 s swell, breaking an ice sheet of 2.0 m thickness into floes 30 m in diameter, will lose $\approx 30\%$ of its energy after travelling through only one kilometre of newly broken ice, and almost 50% over a distance of two kilometres. For this reason, fast ice will tend to break out in stages, with any given incident swell being able to cause fracturing only a short distance into the ice covered region. Once the 'debris' is dispersed by wind or currents the breakup process can begin again as soon as the incident wave amplitudes reach a_0^*. Only when the amplitude of the swell is far in excess of a_0^* will large scale, wave-induced breakouts be possible.

A limited breakout of this nature was observed in McMurdo Sound, near the Erebus Glacier Tongue, on February 11, 1986. During helicopter flights from Scott Base to Cape Evans on February 10 and 11, the author (GBC) observed roughly two kilometres of fast ice breaking up into floes roughly 30 m wide, and between 30 and 100 m in length (Fig. 11). Also, a series of twelve parallel cracks, running perpendicular to the direction of the swell, were seen at ≈ 30 m intervals in the as yet unbroken section of the ice sheet. From the MV "Polar Queen" (seen in the photograph) the swell was estimated to have an amplitude of between 0.1 and 0.2 m, and was noted as being "long period", although the exact frequency was unfortunately not recorded. Referring to Fig. 4, swell of this amplitude is in excess of the predicted critical value for all wave periods except 5 s, suggesting that the calculations are roughly of the correct magnitude. The attenuating effect of the newly created floe field was clearly evident, and no further fracturing occurred; in fact this event constituted the last major breakout in McMurdo Sound until early June, when extremely strong local winds

Fig. 11. Photograph of the fast ice breakup in McMurdo Sound on February 11, 1986. The view is toward the northeast with Mount Erebus in the background and the MV "Polar Queen" in the left of the frame (photograph courtesy of M. Harman).

resulted in the destruction of a large area of ice along the western side of the Sound.

BREAKUP BY WIND AND WATER STRESS

Fast ice sheets can also be broken up by the horizontal stresses resulting from wind drag at the upper surface and water drag at the lower surface. A general equation for shear stress caused by both wind and currents can be written as:

$$\tau = C_D \rho_x u^2 \tag{27}$$

where ρ_x is the fluid density (air or water), and C_D is the surface drag coefficient. Values for C_D are derived from wind and current velocity profiles, and are products of both skin friction and form drag. Drag coefficients measured in the Arctic, where the ice is typically much rougher than in the Antarctic, normally range from 1×10^{-3} to 3×10^{-3} for air (Overland, 1985), and 1×10^{-3} to 8×10^{-3} for water (Mellor, 1983). Possible modes of shear stress induced failure include crushing, tension, and buckling, but because the average normal stresses are small, an ice sheet will fracture only if the wind or current acts over very large distances. The minimum fetch (l_{min}) required to cause crushing or tensile failure is:

$$l_{min} = \frac{\sigma_x^* h_i}{\tau} \tag{28}$$

where σ_x^* is the ice strength (in crushing or tension). For a fast ice sheet of fixed horizontal extent, the critical wind or water velocity required for failure is:

$$u_{crit} = \left(\frac{\sigma_x^* h_i}{C_D \rho_x l}\right)^{1/2} \tag{29}$$

Failure may also occur by buckling, which yields the analogous formula:

$$u_{crit} = \left(\frac{F_b}{C_D \rho_x l}\right)^{1/2} \tag{30}$$

where the buckling force (F_b) is (Ashton, 1986):

$$F_b = \left(\frac{\rho_w g E h_i^3}{12(1-\nu^2)}\right)^{1/2} \tag{31}$$

Since ice is unlikely to buckle under true elastic conditions, the value used for Young's modulus (E) in Eq. 31 should be less than the true value (Mellor, 1983).

For simplicity, the quantities σ_c and σ_t will be derived from the empirical equations (Weeks and Assur, 1967):

$$\sigma_c = 1.65\times10^6\{1-(\nu_b/0.275)^{1/2}\} \tag{32}$$

and (Dykins, 1971):

$$\sigma_t = 8.20\times10^5\{1-(\nu_b/0.142)^{1/2}\} \tag{33}$$

A review and assessment of these and other experimentally derived formulae can be found in Schwarz and Weeks (1977).

Setting l to 50 km (the maximum extent of the fast ice sheet in McMurdo Sound), C_D to 5×10^{-3}, at the upper limit of drag coefficients (Langleben, 1972; Banke and Smith, 1973; Overland, 1985; Ashton, 1986), and all other parameters as previously defined, the temporal variations in u_{crit} can then be determined (Figs. 12 and 13). In Fig. 12 the dotted line at 45 m s^{-1} represents an approximate maximum expected wind velocity. This value,

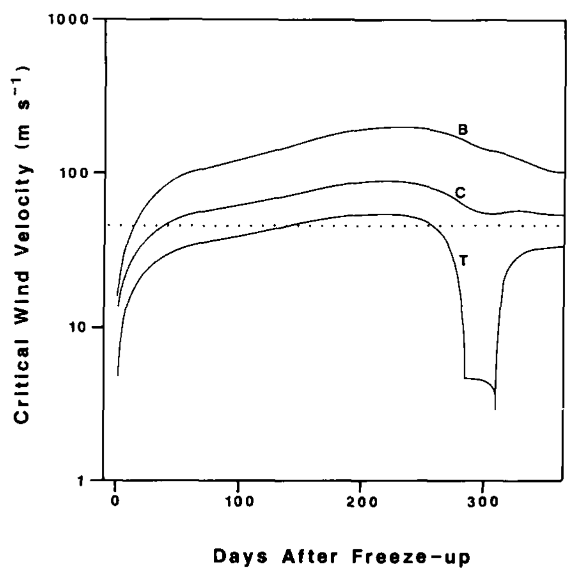

Fig. 12. Seasonal variations in the critical wind velocity (u_{crit}) for buckling (B), compressive (C), and tensile (T) failure of McMurdo Sound fast ice. The dotted line at 45 m s^{-1} represents an approximate maximum expected wind velocity for the region.

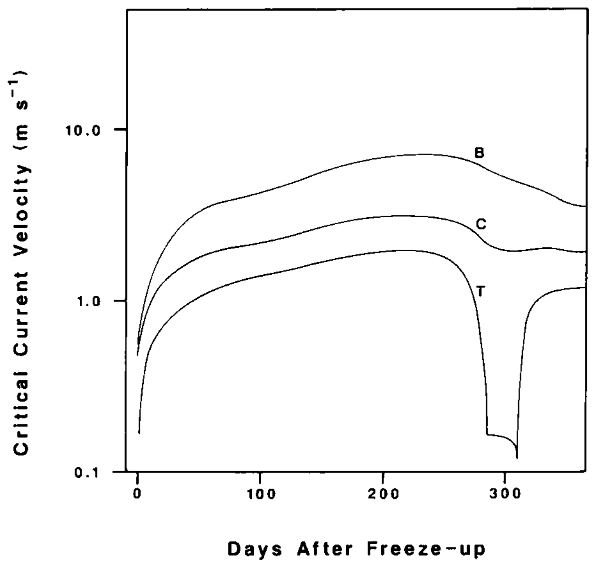

Fig. 13. Seasonal variations in the critical current velocity for buckling (B), compressive (C), and tensile (T) failure of McMurdo Sound fast ice.

although not unreasonable, is probably an overestimate. The maximum gust observed at Scott Base during 1986 was roughly 42 m s^{-1}, and the maximum mean wind speed over a period of at least 25 minutes was about 33 m s^{-1}, where 25 minutes is the time required for a parcel of air to travel 50 km at 33 m s^{-1}. The unusual drop in u_{crit} for tensile failure in summer is due to the inadequacy of the empirical formula (Eq. 33) in representing σ_t at very high brine volumes, but although the exact shape of the curve at this point is questionable, the general pattern of a large decrease can be considered real. The graph shows that buckling by elastic instability is unlikely to occur except when the ice is extremely thin, a general conclusion also reached by Mellor (1983). An alternative analysis by Kerr (1980) suggests that a semi-infinite floating ice sheet could buckle under smaller forces than predicted by conventional theory, although at the present time the magnitude of this effect cannot be estimated (Mellor, 1983).

Failure by compressive stress is also limited to periods when the ice cover is thin, and is made even more improbable in this specific area by the requirement for strong winds from northerly quadrants, which are rare. Failure in tension however, is more plausible. The analysis indicates that during much of the year the local wind speed might equal or exceed u_{crit}, with mid-winter being the only period when tensile failure seems unlikely. As the input data controlling Eq. 29 (i.e. C_D and l) have been selected so as to minimize u_{crit}, and the dotted line in Fig. 13 is a high estimate of the maximum expected wind velocity, the conclusion that wind stress alone is not likely to induce breakup in mid-winter appears sound.

In Fig. 12 the critical water velocities show essentially the same characteristics, but at vastly different magnitudes. It is difficult to set a maximum expected current velocity for McMurdo Sound, as the few measurements which are available display considerable variation. In general, the currents have been found to be fairly weak ($\approx$0.1 m s^{-1}), tidally influenced, and exhibiting a complex flow pattern (Gilmour et al., 1962; Tressler and Ommundsen, 1962; Gilmour, 1975; Lewis and Perkin, 1985); however maximum velocities approaching 1.0 m s^{-1} have been observed (Heath, 1977). Variations in this range are crucial to the problem of tensile failure since a current velocity of 0.2 m s^{-1} produces a shear stress of only about 1% of the mid-winter tensile strength, but at speeds of 1.0 m s^{-1} reaches about 40% of σ_t, such a large increase being attributable to the high density of the fluid. If currents of the order of 1 m s^{-1} are present on a regular basis then water stress must be considered an important contributor to in-plane stress, and possibly breakup, even if it cannot by itself produce sufficient stress to induce fracture. However the complex nature of flow in McMurdo Sound, and the conspicuous absence of similar high velocities in other studies suggest that current speeds this large are rare, or of only local importance.

Having suggested that none of the fracture mechanisms proposed thus far are capable of causing breakup during mid-winter, it is difficult to explain observed mid-winter breakouts such as that which occurred in early June, 1986, when the removal of a large section of fast ice along the western side of McMurdo Sound was observed, and coincided with a period of strong southerly winds on June 6th and 7th, with gusts up to 42 m s^{-1}. This implies that two or more processes must act together to generate the necessary forces, or that there are other processes, not yet considered, which contribute to the breakup of the ice sheet. An additional process which may be important is the direct generation of propagating flexural-gravity waves by turbulent winds blowing across the ice surface (Crocker and Wadhams, 1988).

BREAKUP BY WIND GENERATED WAVES

The McMurdo Sound measurements have shown that propagating flexural-gravity waves can be generated in a fast ice cover by turbulent air flow across the ice surface. Over the range of wind velocities and ice conditions encountered in McMurdo Sound, the waves produced were of insufficient magnitude to induce fracture, but because of the limited range of conditions (ice thickness and fetch in particular), and the uncertainties surrounding the exact nature of the wind/ice coupling, it is difficult to extrapolate from these findings to other situations, and derive a generally applicable relationship. There is however, sufficient information to allow some aspects of the wind/ice coupling to be characterized.

As the measurement site was roughly 5 km from the McMurdo Ice Shelf to the south, and 1.5 km from Pram Point to the north, winds blowing from the two directions provide data sets from two distinctly different fetches. Assuming that wave induced strain is zero when the fetch is zero, these three points can be used to investigate the general nature of the fetch/wave height relationship. Taking only those events where there was sufficient wave energy to produce meaningful spectra (see Crocker, 1988), there are twelve data sets representing southerly winds and four data sets representing northerly winds, all in the velocity range 15–17 m s^{-1}. Knowing that wind-waves in an open sea increase in height h_w in proportion to the square root of the fetch l (Sverdrup et al., 1942; Defant, 1961), we might anticipate that an equation of the form:

$$h_w = cl^{1/2} \tag{34}$$

could be used to characterize the relationship for ice-coupled waves as well. In fact, setting the constant c to 5.8×10^{-4}, produces reasonable association with the limited observations (where l is in kilometres), as shown in Fig. 14. Also shown in the figure are the means and standard deviations of the measured wave heights in the velocity band defined above. Although the mean values of h_w fall close to the theoretical curve, the scatter is so large that the data cannot be used to either support or refute a relationship with $l^{1/2}$ (the mean values of h_w also fall very close to a straight line). It can be said however, that there is a significant increase in h_w with the fetch increase of 3.5 km.

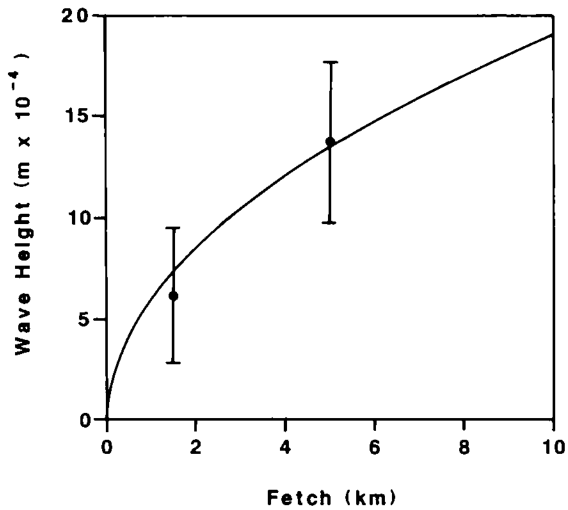

Fig. 14. Means and standard deviations of the observed wave heights for wind velocities between 15 and 17 m s^{-1} and the two different fetches. Also shown is the wave height/fetch relationship predicted using Eq. 34.

Estimating the size of wind-generated waves in ice sheets of different thicknesses than those observed at the main sampling site is equally difficult. Crocker (1988) discusses this problem in some detail, but the likelihood of feedback mechanisms between the turbulent pressure fluctuations producing the waves and the motions of the ice make it extremely difficult to predict how different ice sheets will respond to a given forcing. At the present time we cannot make any definitive statements, but recognize that in certain situations wind generated ice-coupled waves may play an important role in ice sheet breakup.

DISCUSSION AND CONCLUSIONS

Throughout most of the year several of these forces will be acting on the ice sheet at any one time, and although a single mechanism may be dominant during specific breakup events, it is most likely that there will be more than one contributing process. In the absence of a pack ice cover in the Ross Sea during the summer, ocean swell is easily capable of causing breakup, and as such events are frequently observed when local winds are slight, it is clear that wave induced fracture dominates at this time of year. In the winter however, it has been found that only *very* extreme (and in some cases unreasonably large) winds, currents, and waves can generate the forces required to fracture the ice, suggesting that the combined effects of several stress inducing mechanisms are needed. The roles played by ocean swell and currents in contributing to winter breakouts appear to be minor, leaving wind stress as the dominant force, with wind generated waves remaining for the most part an unknown quantity. Uncertainties in the exact nature of wind-wave formation make it difficult to predict exactly how they might act in conjunction with tensile stress. Kerr's (1983) analysis indicates that horizontal (or 'in-plane') stress modifies the propagation characteristics of waves in a floating, continuous ice sheet. In tension, the phase velocity increases, implying that increasing wind stress would result in reduced wave-induced strain. As yet Kerr's theory has not been adequately tested and we cannot say if the effect is significant, only that this is another problem which requires further field, or perhaps laboratory, investigations.

The preceding analysis suggests that the extent of the summer breakout in McMurdo Sound is controlled largely by the pack ice conditions in the Ross Sea. If this is correct, then we would expect to find substantiating evidence in the 30 years of ice observations from the region. However, finding a numerical relationship between pack ice "conditions" and fast ice "extent" is difficult because neither can be easily quantified. For instance, the total sea surface area covered by pack ice might seem to be a representative statistic, but problems arise in situations where special spatial or temporal distributions become important. Cases where the Ross Sea is generally ice free near Ross Island but contains an extensive pack ice belt several hundred kilometres to the north, or where a corridor of open water briefly appears in an otherwise close pack ice cover (as examples), may permit extensive fast ice breakouts while the average pack ice concentration is high. The situation is further complicated by the requirement that the ice-free sea must coincide with sufficiently large incident swell, the latter being controlled by weather systems in the Southern Ocean and therefore very difficult to predict.

A more practicable approach is to use a simple qualitative analysis, such as that employed by Preeble (1968). By considering a variety of ice conditions contributing to swell attenuation Preeble developed general descriptive classifications for the severity of the pack ice conditions, and compared them with observed fast ice breakouts over the years 1955–1966. The results (his table 1, p. 918) clearly demonstrate the tendency for heavy pack ice years to be accompanied by very limited fast ice breakouts, and for the extensive breakouts to occur during periods of light ice cover in the Ross Sea, supporting the theoretical analyses described above. This means that in order to develop a more versatile model which predicts the probability of breakup at any given time of year, we must first be able to predict the pack ice conditions in the Ross Sea, as well as the probabilities of critical incident wave amplitudes and local wind and current velocities. At the present time there is insufficient information to perform such an analysis; however, it is hoped that current studies incorporating the effects of thermal deterioration and melting of fast ice sheets will make it possible to produce a model which is representative of fast ice in general, including ice along more northerly sections of the Antarctic coastline, and in Arctic waters.

ACKNOWLEDGEMENTS

This project was supported by the Natural Environment Research Council of Great Britain under grant GR3/5713A. GBC was supported in Cambridge by the National Science and Engineering Research Council of Canada, and in the Antarctic by the Antarctic Division of the New Zealand Department of Scientific and Industrial Research. We thank Dr Andrew Assur for pointing out the erroneous exponent in the Young's modulus equation of Schwarz and Weeks (1977). The assistance of the

1986 winter-over crew at Scott Base is gratefully acknowledged.

REFERENCES

Anderson, D.L., 1958. Preliminary results and review of sea ice elasticity and related studies. Trans. Eng. Inst. Canada, 2(3): 116–122.

Ashton, G.D., 1986. River and Lake Ice Engineering. Water Resources Publications, Littleton, Colo.

Assur, A., 1963. Break-up of pack ice floes. In: W.D. Kingery (Editor), Ice and Snow. MIT Press, Cambridge, Mass., pp. 335–347.

Bagnold, R.A., 1947. Sand movement by waves: some small scale experiments with sand of very low density. Trans. Am. Geophys. Union, 30: 444–469.

Banke, E.G. and Smith, S.D., 1973. Wind stress on Arctic sea ice. J. Geophys. Res., 78 (33): 7871–7883.

Carter, D., Oullett, Y. and Pay, P., 1981. Fracture of a solid ice cover by wind-induced or ship generated waves. In: Proc. 6th Int. Conf. Port and Ocean Engineering Under Arctic Conditions, Québec, 2: 843–856.

Cox, G.F.N. and Weeks, W.F., 1974. Salinity variations in sea ice. J. Glaciol., 13(67): 109–120.

Crocker, G.B., 1988. Physical processes in Antarctic landfast sea ice. Unpubl. Ph.D. thesis, Univ. Cambridge.

Crocker, G.B. and Wadhams, P., 1988. Observations of wind generated waves in Antarctic fast ice. J. Phys. Oceanogr., 18(9): 1292–1299.

Crocker, G.B. and Wadhams, P., 1989. Modelling Antarctic fast ice growth. J. Glaciol., 35 (119): 3–8.

Defant, A., 1961. Physical Oceanography, 2. Pergamon Press, London.

Dykins, J.E., 1971. Ice engineering — material properties of saline ice for a limited range of conditions. U.S. Navy Civil Eng. Lab., Port Hueneme, Tech. Rep. R720.

Frankenstein, G. and Garner, R., 1967. Equations for determining the brine volume of sea ice from $-0.5°$ to $-22.9°C$. J. Glaciol., 6(48): 943–944.

Gilmour, A.E., 1975. McMurdo Sound hydrological observations, 1972–1973. N. Z. J. Mar. Freshwater Res., 9(1): 75–95.

Gilmour, A.E., MacDonald, W.J.P. and Van der Hoeven, F.G., 1962. Winter measurements of sea currents in McMurdo Sound. N. Z. J. Geol. Geophys., 5: 778–789.

Goodman, D.J., Wadhams, P. and Squire, V.A., 1980. The flexural response of a tabular ice island to ocean swell. Ann. Glaciol., 1: 23–27.

Heath, R.A., 1977. Circulation across the ice shelf edge in McMurdo Sound, Antarctica. In: M.J. Dunbar (Editor), Polar Oceans. Proc. Polar Oceans Conf., held at McGill Univ., Montréal, Que. (May 1974), pp. 129–150.

Kerr, A., 1980. On the buckling force of floating ice plates. In: P. Tryde (Editor), Physics and Mechanics of Ice. Berlin, Springer, pp. 163–178.

Kerr, A., 1983. The critical velocities of a load moving on a floating ice plate that is subjected to in-plane forces. Cold Reg. Sci. Technol., 6(2): 267–274.

Langleben, M.P., 1972. A study of the roughness parameters of sea ice from wind profiles. J. Geophys. Res., 77(30): 5935–5944.

Lewis, E.L. and Perkin, R.G., 1985. The winter oceanography of McMurdo Sound, Antarctica. In: S.S. Jacobs (Editor), Oceanology of the Antarctic Continental Shelf. Washington, D.C., Am. Geophys. Union, Antarctic Res. Ser., 43: 145–165.

Liu, A.K. and Mollo-Christensen, E., 1988. Wave propagation in a solid pack ice. J. Phys. Oceanogr., 18(11): 1702–1712.

Mellor, M., 1983. Mechanical behaviour of sea ice. Cold Reg. Res. Eng. Lab., Monogr. 83-1, Hanover, N.H.

Mognard, N.M., Campbell, W.J., Cheney, R.E. and Marsh, J.G., 1983. Southern Ocean mean monthly waves and surface winds for winter 1978 by Seasat radar altimeter. J. Geophys. Res., 88(C3): 1736–1744.

Overland, J.E., 1985. Atmospheric boundary layer structure and drag coefficients over sea ice. J. Geophys. Res., 90(C5): 9029–9049.

Panov, V.V. and Fedotov, V.I., 1979. Physical conditions of fast ice formation in East Antarctica. Polar Geogr. Geol., III(1): 1–15.

Pierson, W.J. and Moskowitz, L., 1964. A proposed spectral form for fully-developed wind seas based on the similarity theory of S.A. Kitaigorodskii. J. Geophys. Res., 69(24): 5181–5190.

Preeble, M.M., 1968. Ice breakout, McMurdo Sound, Antarctica. N. Z. J. Geol. Geophys., 11(4): 908–921.

Putnam, J.A. and Johnson, J.W., 1949. The dissipation of wave energy by bottom friction. Trans. Am. Geophys. Union, 30: 67–74.

Schwarz, J. and Weeks, W., 1977. Engineering properties of sea ice. J. Glaciol., 19(81): 499–530.

Semtner, A.J., 1976. A model for the thermodynamic growth of sea ice in numerical investigations of climate. J. Phys. Oceanogr., 6(3): 379–389.

Squire, V.A., 1984. A theoretical laboratory and field study of ice-coupled waves. J. Geophys. Res., 89(C5): 8069–8079.

Squire, V.A., Langhorne, P.J., Robinson, W.H., Heine, A.J. and Haskell, T.G., 1987. Moving loads on sea ice. Polar Rec., 23(146): 569–575.

Sverdrup, H.U., Johnson, M.W. and Fleming, R.H., 1942. The Oceans. Englewood Cliffs, N.J. Prentice-Hall

Tressler, W.L. and Ommundsen, A.M., 1962. Seasonal oceanographic studies in McMurdo Sound, Antarctica. U.S. Navy Hydrographic Office, Tech. Rep., TR-125, Washington, D.C.

Wadhams, P., 1973a. Attenuation of swell by sea ice. J. Geophys. Res., 78(18): 3552–3563.

Wadhams, P., 1973b. The effect of a sea ice cover on ocean surface waves. Unpubl. Ph.D. thesis, Univ. Cambridge, 223 pp.

Wadhams, P., 1980. Ice characteristics in the seasonal ice zone. Cold Reg. Sci. Technol., 2(1): 37–87.

Wadhams, P., 1986. The seasonal ice zone. In: N. Untersteiner (Editor), The Geophysics of Sea Ice. Plenum Publ. Corp., New York, N.Y., pp. 825–991.

Wadhams, P., Lange, M.A. and Ackley, S.F., 1987. The ice thickness distribution across the Atlantic sector of the Antarctic Ocean in mid-winter. J. Geophys. Res., 92(C13): 14535–14552.

Weeks, W.F. and Assur, A., 1967. The mechanical properties of sea ice. Cold Reg. Res. Eng. Lab., Part II: Physical science, Section C: Physics and Mechanics of Ice, Hanover, N.H.

Zwally, H.J., Comiso, J.C., Parkinson, C.L., Campbell, W.J., Carsey, F.D. and Gloersen, P., 1983. Antarctic Sea Ice, 1973–1976: Satellite Passive Microwave Observations. Washington, Natl. Aeronaut. Space Adm., SP-459.